

# EXPERIMENTAL STUDY OF CHARACTERISTICS OF MICRO-HOLE POROUS SKINS FOR TURBULENT SKIN FRICTION REDUCTION

Danny P. Hwang  
National Aeronautics and Space Administration  
Glenn Research Center  
Cleveland, Ohio, U.S.A.

**Keywords:** *skin friction reduction, porous skin, micro-blowing*

## Abstract

*Characteristics of micro-hole porous skins for the turbulent skin friction reduction technology called the micro-blowing technique (MBT) were assessed experimentally at Mach 0.4 and blowing fractions from zero to 0.005. The objective of this study was to provide guidelines for the selection of porous plates for MBT. The hole angle, pattern, diameter, aspect ratio, and porosity were the parameters considered for this study. The additional effort to angle and stagger the holes was experimentally determined to be unwarranted in terms of skin friction benefit; therefore, these parameters were systematically eliminated from the parametric study. The impact of the remaining three parameters was evaluated by fixing two parameters at the reference values while varying the third parameter. The best hole-diameter Reynolds number was found to be around 400, with an optimum aspect ratio of about 6. The optimum porosity was not conclusively discerned because the range of porosities in the test plates considered was not great enough. However, the porosity was estimated to be about 15 percent or less.*

## 1 Symbols

$A$  area of test plate  
 $C_f$  total skin friction coefficient, (skin friction force)/(1/2  $\rho_\infty u_\infty^2 A$ )  
 $D$  diameter of blowing hole, mm  
 $F$  blowing fraction, ( $\rho_b v_b$ )/( $\rho_\infty u_\infty$ )

$H$  shape factor (i.e., ratio of displacement thickness to momentum thickness)  
 $L$  plate thickness, mm  
 $L/D$  aspect ratio  
 $u_\infty$  free-stream velocity at the leading edge of the test plate, m/sec  
 $v_b$  blowing air velocity, m/sec  
 $\rho_\infty$  free-stream density at the leading edge of the test plate  
 $\rho_b$  blowing air density

## 2 Introduction

One of the interesting challenges in aerodynamics is the development of technology to reduce turbulent skin friction. Many techniques and methods have been tried, as summarized in references [1] and [2]. However, the predicted skin friction levels have not been achieved in practice.

An innovative way to reduce turbulent skin friction, called the micro-blowing technique (MBT), was invented in 1994, and a patent was issued in 1998 [3]. The term ‘micro’ implies that (1) the hole diameters are substantially less than the boundary layer thickness and (2) the blowing flow rate is a very small fraction of the boundary-layer flow rate. In this unique concept, air is blown vertically through a specially designed porous plate with micro-holes at blowing fractions of the order  $10^{-3}$ . The micro-blowing air changes the characteristics of flow over the treated wall, which decreases skin friction beneath fully developed turbulent

boundary layers. Surface smoothness, which is a critical factor for laminar flow control, is not an issue for MBT.

Many proof-of-concept experiments for MBT were conducted over the past 5 years [4–9]. Test results showed that this technique could reduce turbulent skin friction by up to 50 to 70 percent below that of a nonporous solid flat plate in subsonic flow [4] and by up to 90 percent in supersonic flow [8]. These tests showed that successful achievement of skin friction reduction depends strongly on the MBT skin—especially the hole size, aspect ratio, and porosity. In this paper, the characteristics of specially designed micro-hole skins are assessed for subsonic flow conditions, and the relationship between the hole parameters and the turbulent skin friction reduction will be presented. The experiment is described first, followed by related discussion. The final section summarizes the paper.

### 3 Experiment Descriptions

#### 3.1 Wind Tunnel

The Advanced Nozzle and Engine Components Test Facility (CE22) [10] was modified for MBT experiments. A rectangular duct 20.32 cm wide, 14.2 cm high, and 63.5 cm long replaced the usual test article (typically a nozzle) to form a small wind tunnel. A 12.7-cm-long transition duct was used to connect the test section to the facility. The facility provided stable Mach numbers from 0.35 to 0.7 at the static pressure of 0.24 atm (the ambient static pressure at 35,000 ft altitude). The exhaust pressure at the exit of the test section could be adjusted from 1.0 atm to near vacuum, and the supply total pressure could be as high as 2.7 atm.

#### 3.2 Experiment Setup and Instrumentation

A 12.36- by 25.06-cm test plate was placed in a rectangular opening on the tunnel floor with a small gap of 0.18 mm between the plate and the tunnel floor. The test plate surface was flush with the tunnel floor. The leading edge of the test plate was 25.4-cm downstream from the end

of the transition duct. The test plate was firmly held by a plate frame holder, which was bolted directly onto a force balance. Two different balances were used for the study: a one-component balance [11] and a two-component balance that was built by an outside manufacturer. A load cell with a maximum loading of 500 g and an accuracy of  $\pm 0.25$  percent was used for the one-component balance. Load cells of 11 340 g and accuracies of  $\pm 0.025$  percent or better were used for the two-component balance. This balance can measure both compressive and expansive forces. Even with a larger load cell, the two-component balance had an accuracy similar to that of the one-component balance. The balance was placed under the test section inside a sealed compartment to minimize air leakage through the gap between the plate and the tunnel floor.

A total pressure rake was placed at the centerline on the tunnel floor. This rake was built of tubing with openings 1.27-cm upstream of the trailing edge of the plate with a very small vertical gap of less than 0.2 mm between the test plate and the nearest tube. The outside diameter of the tubing was 0.508 mm. The total pressure rake was used to calculate the momentum thickness and the velocities inside the boundary layer. A total pressure probe, a static pressure probe, and a total temperature thermocouple were placed at the entrance of the plate on the top surface of the tunnel for a free-stream Mach number measurement. There were 24 static pressure probes along the centerline on the top surface of the wind tunnel. An electronic mass flow meter, with a size of 1500 SLM (standard liters per minute), was used to measure the flow rate of the blowing air.

#### 3.3 Calibration

For the one-component balance, an identical load cell was used to calibrate the load cell inside the balance. The calibration showed that the friction of the balance was very small because frictionless flexural pivots were used. The data were adjusted during the data acquisition process for this small difference.

For the two-component balance, a push-pull calibration using a pneumatic calibration

system on the balance was used. It gave a very consistent calibration slope of about 1.008.

### 3.4 Test Matrices and Skins Tested

The test was conducted for four Mach numbers (0.4, 0.5, 0.6, and 0.7). The Reynolds numbers per meter were  $2.2 \times 10^6$  to  $4.3 \times 10^6$ . The blowing fraction varied from 0 to 0.005. The specifications of all the porous plates are listed in Table I, and pictures of some example micro-hole porous plates are shown in Fig. 1. The stainless steel test plates were designed by NASA and fabricated by an outside manufacturer. The holes were laser-drilled.

The PN23 plate was selected as the reference porous plate, with a hole diameter of 0.17 mm, an aspect ratio of 6.2, and a porosity of 23 percent. All other porous plates were fabricated by changing only one of the parameters from this plate. In some test plates, slight differences in the fixed parameters exist because a standard thickness plate had to be used.

## 4 Results and Discussion

The exit tunnel pressure was fixed at 0.24 atm for the results presented herein, and the total temperature of the tunnel and blowing air was

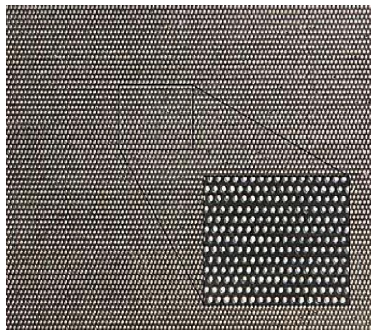
near 530 °R. The turbulence intensity of the tunnel was not measured but is believed to be high and the shape factor obtained from the flat plate tests was about 1.34. Therefore, the flow over the test plate is considered to have been highly turbulent. The exhaust vacuum air was shared with many facilities, and occasional fluctuations in mean flow variables were measured whenever a user demanded air in an adjacent test cell. The blowing fraction was varied from 0 to 0.005, and Mach numbers were varied from 0.4 to 0.7. The normalized results were similar at all Mach numbers; therefore, only Mach 0.4 is presented herein.

In a typical series of tests, solid flat plates were first tested to establish reference values for skin friction (shown in Fig. 2). Because of the boundary layer buildup inside the duct, the static pressure was slightly lower at the trailing edge than that at the leading edge of the test plate. Unfortunately, the effect of the pressure loading on the balance was not tared out of the results. Therefore, the data obtained from the test were slightly higher than those for the theory of Ludwig and Tillman [12], also presented in Fig. 2. A comparison of the measurements from many years of testing using the different balances, is shown in Fig. 3 for the

TABLE I.—TEST PLATE SPECIFICATIONS

Plate name	Porosity, percent	Hole diameter $D$ , mm	Skin thickness, $L$ , mm	Aspect ratio, $L/D$	Hole angle from normal, deg	Pattern
PN4	23	0.1651	1.016	6.15	5	Staggered
PN5					15	Staggered
PN6					5	Aligned
PN7					15	Aligned
<sup>a</sup> PN23	▼	▼	▼	▼	0	Staggered
PM1	13	.1803	1.163	6.45		
PP1	33	.1803	1.163	6.45		
DM1	23	.066	.432	6.54		
DP1	23	.29	1.864	6.44		
ARM1	23	.1803	.574	3.23		
ARP1	23	.16	1.473	9.21		
PP2	43	.1803	1.163	6.45		
DP2	23	.523	3.353	6.41	▼	▼

<sup>a</sup>PN23 is the reference plate.



PN23 top view



PN23 cross section



PN5 cross section

Fig. 1.—Closeup pictures of micro-hole porous plates.

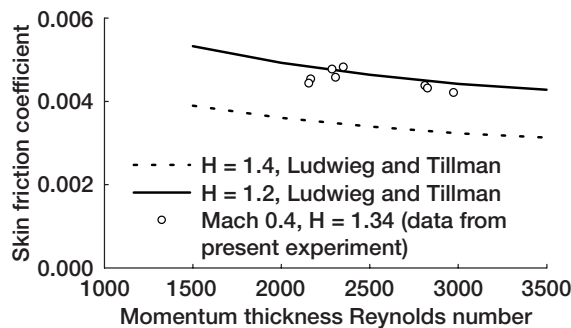


Fig. 2.—Measured skin friction coefficient of flat plate compares well with theory.

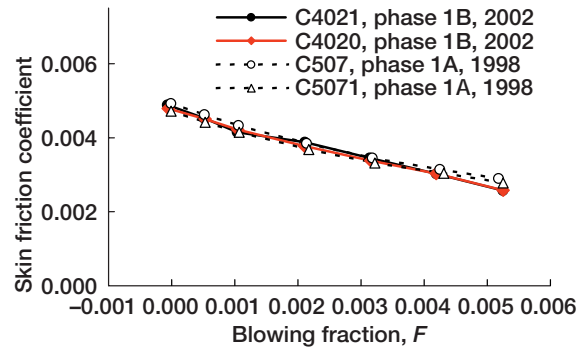


Fig. 3.—Skin friction coefficient of PN23 (reference) plate.

micro-blown PN23 porous plate. Excellent repeatability can be seen in this figure (i.e.,  $\Delta C_f/C_f \cong 5$  percent).

Five hole parameters were considered in this study: angle, pattern, diameter, aspect ratio, and porosity (percentage of open area). A sensitivity study was first carried out to eliminate the hole parameters that have minimal impact on skin friction reduction.

#### 4.1 Sensitivity Study of Hole Angle and Pattern

The effect of hole angle (measured with respect to the normal to the plate surface) is presented in Fig. 4. Using an angle of  $15^\circ$  only provided an additional 5- to 6-percent reduction in skin friction in comparison to the friction of straight vertical holes. The additional cost associated with the fabrication of porous plates with angled holes could not be justified by this small improvement in skin friction reduction. Therefore, the hole-angle parameter was eliminated

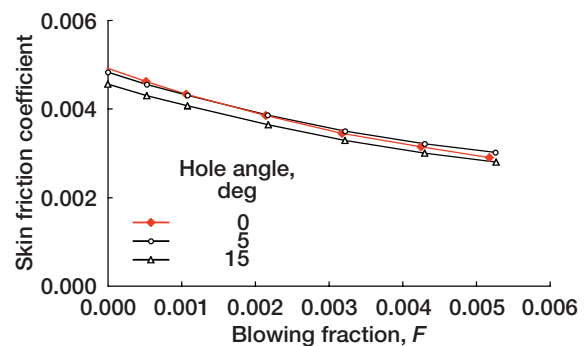


Fig. 4.—Effect of hole angle on skin friction reduction.

from the study. Note, however, that the benefit of angled holes is apparently independent of the blowing fraction and that it is related instead to the decrease in the effective roughness as the hole angle is increased.

Schematic diagrams of staggered-hole and aligned-hole patterns are given in Fig. 5. It is clear from the data shown in Fig. 6 that the effect of hole pattern was small for the 5° angle test plates, whereas the skin friction of the staggered pattern with 15° holes was 8-percent

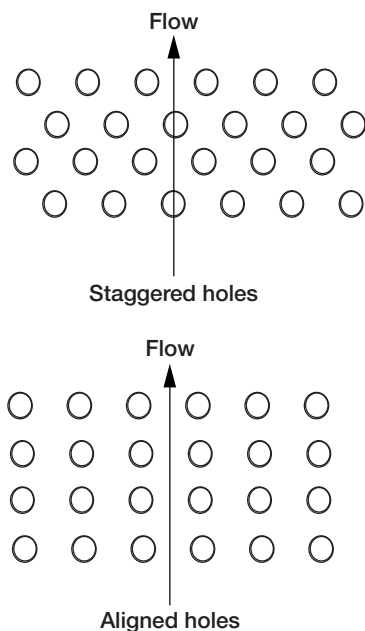


Fig 5.—Schematic diagrams of hole patterns

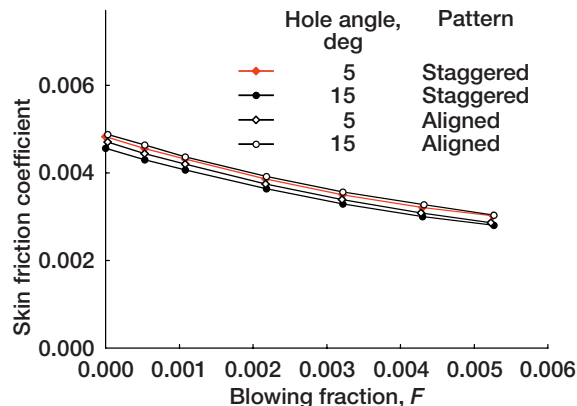


Fig. 6.—Effect of hole pattern on skin friction reduction.

lower than that of the aligned hole pattern. It was concluded that there might be some marginal benefit derived by optimizing the hole pattern but that the benefit would be small for 0° holes, which most likely would be used in practice. Therefore, pattern differences were also eliminated from the study.

A series of micro-porous plates were designed and fabricated with the remaining parameters—hole diameter, aspect ratio, and porosity. Only one of the remaining hole parameters was varied from the PN23 value in each plate. The impact of these three parameters is shown in Figs. 7 to 9.

#### 4.2 Impact of Diameter

The effect of hole diameter is shown in Fig. 7, which gives the test results from the porous plates: PN23, DM1, DP1, and DP2. The skin friction with zero blowing (unblown skin friction) is the measurement of the skin friction including the effective roughness of the micro-holes. The ratio of the skin friction coefficient of the porous plate to that of a flat plate is called the skin friction ratio. If the ratio is unity, the skin friction of the porous plate is equivalent to that of the solid flat plate. The unblown skin friction ratio (at  $F = 0$ ) for a diameter of 0.523 mm (corresponding to a Reynolds number of 1240) is about 3, as shown in Fig. 7. It was impossible at the achievable blowing fractions to reduce the skin friction of this plate below that of a solid flat plate. Evidently, the unblown

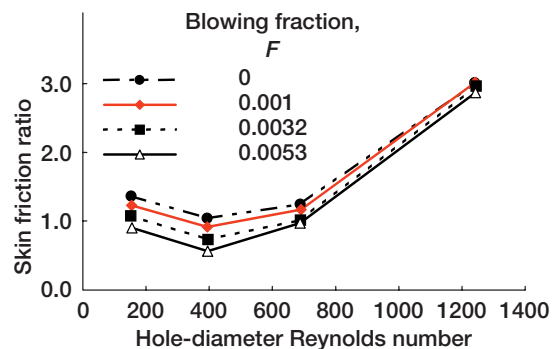


Fig. 7.—Search for minimum value of skin friction ratio with respect to the hole-diameter Reynolds number.



skin friction is a key value to be determined in the selection of the MBT porous plate.

For plates with large holes, it is postulated that, in the zero blowing limit, the boundary layer flow enters the micro-hole and stagnates and, thus, causes an effective plate ‘roughness.’ For a 23-percent porosity to be maintained, the plates with the smallest diameter (0.066 mm) required an extremely large number of micro-holes. The unblown skin friction was high in this limit as well. An optimum hole size was found between these two extreme values, as shown in Fig. 7. A hole-diameter Reynolds number of 400 (corresponding to  $D = 0.17$  mm) was found to be the best hole size in this study.

### 4.3 Impact of Aspect Ratio

Because the hole diameter and porosity were kept as constants (0.17 mm and 23 percent), the impact of aspect ratio on the turbulent skin friction reduction could be investigated using test plates PN23, ARM1, and ARP1, as shown in Fig. 8. Similar to the results from reference [4], the unblown skin friction ratio was very large for the low aspect ratio of 3.23. For plates with a low aspect ratio, it is postulated that, in the zero blowing limit, the boundary layer flow penetrates deeply into the micro-hole and gives rise to large effective plate roughness. For plates with higher aspect ratio, it is also postulated that boundary layer flow cannot penetrate deeply into the micro-hole because of the vortices

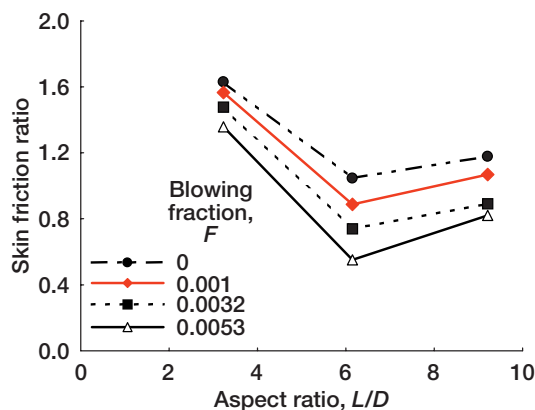


Fig. 8.—Search for minimum value of skin friction ratio with respect to the aspect ratio.

formed inside the hole (similar to the open cavity flow). It is unclear why the unblown skin friction ratio of the aspect ratio of 9.21 was also high. However, from this experiment, the best aspect ratio for MBT was about 6, as shown in Fig. 8.

### 4.4 Impact of Porosity

Four plates, with porosities of 13, 23, 33, and 43 percent (PM1, PN23, PP1, and PP2), were built with hole diameters of 0.17 mm and aspect ratios of 6. Test results are given in Fig. 9. Why the skin friction is much higher at a porosity of 33 percent is unknown. At the fixed hole size, the number of micro-holes was directly proportional to the plate porosity. The skin friction ratio generally increases weakly with increasing porosity (and number of micro-holes). The skin friction reductions at porosities of 13 and 23 percent were very close. Unfortunately, test plates with less than 13-percent porosity were not built for this test. The skin friction of a plate with less than 13-percent porosity could be either higher or lower than that of the 13-percent porosity plate. For real-world applications, fewer holes mean lower manufacturing costs, and therefore, design tradeoffs will involve optimizing hole size and porosity to minimize hole number while maximizing skin friction reduction. For the 0.17-mm holes considered here, the best porosity is estimated to be about 15 percent or less.

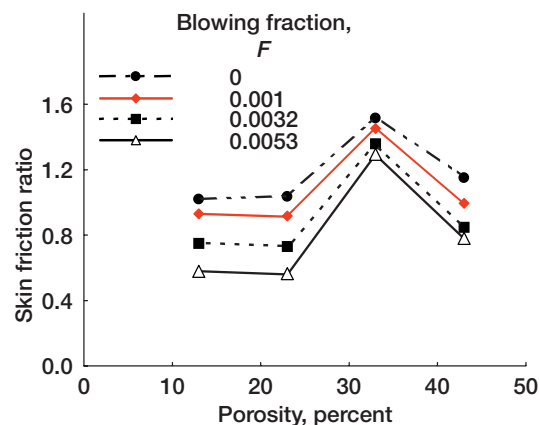


Fig. 9.—Search for minimum value of skin friction ratio with respect to the porosity.

## 5 Concluding Remarks

Experiments to establish the characteristics of micro-hole porous skins for MBT were conducted. The results were presented for Mach 0.4 flow. The following hole parameters were considered: angle, pattern, diameter, aspect ratio, and porosity. Although some improvement can be achieved by hole angle and pattern optimization, these parameters were eliminated from the study because of manufacturing cost considerations. The impact of the remaining three parameters was determined experimentally. It was found from this study that the best hole-diameter Reynolds number was about 400, the best aspect ratio was about 6, and the best porosity was estimated to be 15 percent or less.

## Acknowledgments

This work was funded by the NASA Glenn Research Center's Aerospace Propulsion & Power Base R&T program. The author thanks Tony Hermann who prepared the engineering work for this test. In addition, the following individuals are acknowledged for their contributions during the experiments: Joyel Kerl, Kert Loos, Don Hammett, Kamana Katiyar, Carlos Gomez, and Wayne Stopak.

The author also thanks Jerry Welch for reviewing the final draft and providing valuable comments.

## References

- [1] Bushnell, Dennis M. and Hefner, Jerry N. *Viscous drag reduction in boundary layers*. American Institute of Aeronautics and Astronautics. Washington, DC, 1990.
- [2] *Special course on skin friction drag reduction*. AGARD-R-786, 1992.
- [3] Hwang, Danny P. *Skin friction reduction by micro-blowing technique*. U.S. Patent 5,803,410, Dec. 1995.
- [4] Hwang, Danny P. *A Proof of concept experiment for reducing skin friction by using a micro-blowing technique*. NASA TM-107315 (AIAA Paper 97-0546), 1996.
- [5] Hwang, Danny P. and Biesiadny, Tom J. *Experimental evaluation of the penalty associated with micro-blowing for reducing skin friction*. NASA TM-113174, 1997.
- [6] Hwang, Danny P. Skin-friction reduction by a micro-blowing technique. *AIAA J.*, Vol. 36, No. 3, pp. 480-481, March 1998.
- [7] Tillman, T.G., and Hwang, D.P. *Drag reduction on a large-scale nacelle using a micro-blowing technique*. AIAA Paper AIAA-99-0130, 1999.
- [8] Hwang, Danny P. *An experimental study of turbulent skin friction reduction in supersonic flow using a micro-blowing technique*. AIAA-2000-0545, 2000.
- [9] Welch, Gerard E., et al. *Effectiveness of micro-blowing technique in adverse pressure gradients*. NASA/TM-2001-210690 (AIAA-2001-1012), 2001.
- [10] Beltran, Luis R., Del Roso, Richard L. and Del Rosario, Ruben *Advanced nozzle and engine components test facility*. NASA TM-103684, 1992.
- [11] Voisinnet, R.L.P. *Influence of roughness and blowing on compressible turbulent boundary layer flow; skin friction drag*. NSWC TR-79-153, 1979.
- [12] Schlichting, Hermann *Boundary layer theory*. McGraw-Hill, Inc., New York, NY, 1955, p. 575.